

Research on the influence of the geometric characteristics of surrounding rock fractures on the macroscopic mechanical properties of rock-like materials based on PFC

Xiaoye Zhu

Shandong Normal University, Jinan, China

Abstract. The surrounding rock of coal mining face often contains numerous micro-cracks, and these micro-cracks greatly restrict the mechanical strength of the rock. Mechanical properties of rock degraded by joints and fissures in rock,, taking the Mesozoic three-stream pluton granite in Dandong City, Liaodong uplift area as an example,, establish a particle flow model and use the "trial and error method" to repeatedly calibrate the microscopic parameters until they are consistent with the actual situation,, uniaxial compression tests were performed on rock masses with different fissures, and 16 orthogonal discrete element numerical simulation experiments with 4 factors and 4 levels were carried out. Based on multiple linear regression analysis, the influence of four factors on the mechanical properties of granite was analysed, and the influence of single factor on the macro-mechanical properties of granite was studied through numerical experiments. The results show that the effect of the crack geometry on the peak strength of granite is greater than the effect on the elastic modulus of granite; The order of the influence degree of the crack geometric characteristic parameters on the peak strength is the crack Y-axis position component > the crack X-axis position component > the crack length > the crack inclination angle; The order of the influence degree of the crack geometric characteristic parameters on the elastic modulus is the crack X-axis position component > the crack Y-axis position component > the crack length > the crack inclination angle; The crack initiation position gradually moves to both ends of the crack as the angle increases. The specimen is mainly dominated by tension cracks, and the crack tip is accompanied by local shear failure; The longer the crack length, the lower the peak strength of the granite, and the worse the stability; The positional change of primary microcracks in granite mainly changes the peak strength and post-peak stress-strain state of the rock sample, but has no significant effect on the elastic modulus. The research results have certain reference value for predicting the mechanical properties of fractured granite.

Keyword: Rock mechanics; Particle flow; Microfractures; Peak strength

1. Introduction

In addition to pores, the surrounding rock of the coal mining face usually contains natural cracks or fissures of different sizes (such as faults, joints, micro-cracks, etc.). The existence of these discontinuous surfaces causes the mechanical properties of the rock to deteriorate to varying degrees. Many geotechnical buckling failures are caused by crack/crack propagation inside the rock, and the fracture characteristics and mechanical properties of the cracked rock mass usually determine the peak strength and failure mode of the rock mass. Therefore, it is of great engineering significance to study the relationship between the geometric characteristics of cracks in rock mass, the law of expansion after loading and the macroscopic strength of rock mass.

Many scholars at home and abroad have carried out a large number of uniaxial and triaxial compression

experimental studies on natural rock masses with different lithologies or similar materials containing fractures, and accumulated many rich results in fracture propagation and rock failure in fractured rock masses. Zhang Guokai et al. [1] used high-strength gypsum-like materials to make specimens, used MTS rock mechanics testing machine to conduct uniaxial compression tests on rocks with single fractures, and used acoustic emission, sound waves and camera tests to obtain fracture initiation pressure, peak value. The strength is consistent with the change of the fissure inclination, showing a trend of first decreasing and then increasing. Xiao Taoli et al. [2] used high-strength silica fume mortar to make specimens, and carried out triaxial loading tests under different confining pressures, showing that the peak strength of rock mass will gradually decrease with the increase of single fracture length. Zhou Hui et al. [3] conducted direct shear tests using cement mortar rock materials with prefabricated fractures, and

found that the longer the joint fracture, the lower the shear strength and cohesion of the rock, and for the joint fracture of the same length, its different positions in the rock have very different effects on the strength of the rock. When it is in the middle of the specimen, the shear strength and cohesion of the rock are the smallest, and the peak shear strength and cohesion of the rock are the largest when the joint crack is located at the rear end of the specimen. Liu Hongyan [4] conducted uniaxial compression tests on prefabricated jointed rock masses using similar materials, and found that with the increase of the number of parallel joint groups, the peak strength of the specimen gradually decreased. Ke Zhiqiang et al. [5] used cement mortar and other materials to make columnar jointed rock mass models with different column inclination angles and distribution of lateral joints. And through uniaxial compression test, the influence of column inclination and lateral joints on the anisotropic mechanical properties and failure mechanism of rock mass is studied. It is of scientific value to select materials similar to natural rock mechanics and properties to study rock crack propagation and failure modes. However, due to the proportion of various ingredients and various errors in the experiment, the results of experimental research using similar materials have great uncertainty. Therefore, many scholars use the method of prefabricated fractures in natural rock mass to carry out experimental research on rock mechanical characteristics. Guo Qifeng et al. [6] used GAW2000 rigidity testing machine to conduct uniaxial compression test on prefabricated single-fracture granite samples. It is concluded that the uniaxial compressive strength of the rock sample is the largest when the crack orientation is parallel to the loading direction, and the rock strength decreases with the increasing angle between the crack orientation and the loading direction. Yin Qian et al. [7] used YNS2000 universal servo press to conduct uniaxial compression test on sandstone samples with longitudinal fractures, and studied the effect of strength deterioration of sandstone. It is found that with the increasing of the prefabricated fissure offset, the bearing capacity of the specimen first increases, then decreases, and then increases again, indicating that the position of the fissure has an important influence on the rock failure mode.

With the development of computer numerical simulation technology, the combination of numerical simulation software and laboratory test is an effective method to analyze the failure mode of fractured rock mass. In the aspect of rock mass failure caused by crack propagation in fractured rock mass, the previous studies on cracks mostly focus on a single variable, while the comprehensive variable analysis of cracks shows less impact. Wang et al.[8] used RFPA numerical simulation software for rock fracture process to study the effect of original fracture length on fracture propagation and evolution under specific stress conditions.

2. Numerical model establishment of crack propagation and buckling failure in granite with fissures

The test rock samples were taken from the Sangului rock mass granite quarry in Sangului Village, Dandong City, Liaoning Province. The formation age of granite is Mesozoic, and its main mineral components are quartz, alkaline feldspar, plagioclase, and a small amount of biotite. The rock is unweathered, gray-white on the outside, dense, and has no obvious cracks on the surface, but the permeability test shows that it contains many cracks.



Fig.1 The granite samples obtained from the Sangului rock mass of Dandong city

The granite samples used in the test were cut into the standard size of rock mechanics, that is, $\Phi 25 \text{ mm} \times 50 \text{ mm}$, as shown in Figure 1. Using the MTS815.03 rock triaxial testing machine, the triaxial compression experiments of three rock samples under several different confining pressures (5 MPa, 10 MPa and 20 MPa) were carried out. When the axial loading pressure is continuously increased to cause the rock to become unstable and fail, record the peak stress (that is, the compressive strength of the rock 1). The elastic modulus, cohesion and internal friction angle of the rock were obtained according to relevant calculations (Table 1).

Table 1 Mechanical properties of granite samples obtained from Dandong city

| Samp le serial numb er | E/(GP a) | σ_1/MPa | σ_3/MPa | Cohesi on (MPa) | Intern al fricti on angle (ϕ) |
|------------------------------------|-------------|-----------------------|-----------------------|---------------------------|--|
| 1 5 | 23.46 73 | 242.54 73 | 5 | 19.65 | 62.68 |
| 2 92 | 23.56 92 | 339.00 23 | 10 | | |
| 3 | 26.06 | 498.96 76 | 20 | | |

2.1 Numerical Model Construction

Under the condition of external force, in order to intuitively observe the propagation and evolution of internal cracks, the failure process of rock instability, and the correlation between the geometric characteristics of cracks and the macro-mechanical properties of rock samples, in this paper, relevant numerical experiments are carried out using the particle flow numerical simulation software PFC2D. PFC2D is a numerical simulation software developed by ITASCA based on the principle of

discrete element stress analysis. It is often used to simulate the instability and failure process of rocks, and can be applied to both microscopic damage and macroscopic damage of rock materials. Based on the physical and mechanical properties of granite, domestic and foreign scholars generally use the bonding model to study the instability and failure process of granite. The bonding model is divided into a contact bonding model and a parallel bonding model. The parallel bonding model can transmit forces and moments [9], and is suitable for materials with cement inside the rock, and the cemented part can also simulate the initiation and propagation of cracks. Therefore, the parallel bonding model is suitable for the study of granite cracks. In this paper, the parallel bond model is used as the constitutive model to study the expansion process of the newly-created cracks and the instability failure of the rock samples after the granite with primary cracks is loaded. The two-dimensional geometric model of the standard rock sample in this paper is set to be 100 mm long and 50 mm wide, and the uniaxial compression model is determined by deleting the "walls" on both sides.

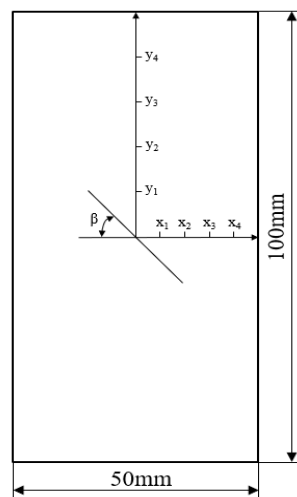


Fig.2 Geometric parameters of single cracked specimen

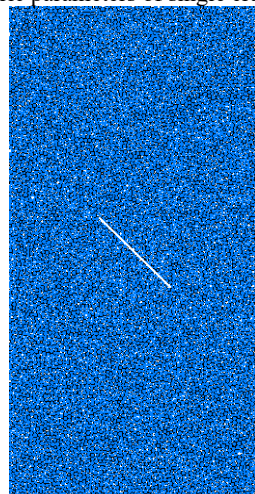


Fig.3 PFC2D simulation of granite particle arrangement

2.2 Microscopic parameters of the parallel bonding model

In the parallel bond model, the macro-mechanical properties of rock (peak strength, Poisson's ratio, elastic modulus) are mainly affected by microscopic parameters such as particle contact modulus, particle stiffness ratio, particle size, particle normal strength, tangential strength, parallel bond contact modulus, parallel bond stiffness ratio, etc[10]. The parallel bonding model has many meso-parameters. In order to reduce the difficulty of calibration, some assumptions are generally made to reduce the number of meso-parameters. The calibration of the meso-parameters is based on multiple laboratory tests, so as to obtain results that are more consistent with the macro-mechanical properties.

When determining the meso-parameters of the parallel bonding model, the following assumptions are followed [11-16]:

1. The uniaxial compressive strength is less than the shear strength, that is, $\sigma < \tau = c + \sigma \tan \phi$, in order to obtain a suitable uniaxial tension-compression ratio.

2. $\gamma = 1.0$

3. $R_{\max}/R_{\min} = 1.66$

4. $\rho = 2830 \text{ kg/m}^3$

5. $\mu = 0.5$

6. $E_p = E_c, k_n/k_s = \bar{k}_n / \bar{k}_s$

The uniaxial compression test is carried out by the particle flow numerical simulation software PFC2D. The microscopic parameters are repeatedly modified by the "trial and error method" by comparing the macroscopic parameters of the indoor test. Finally, the macroscopic mechanical parameters obtained by the uniaxial compression numerical simulation test and the macroscopic mechanical parameters of the laboratory test have an error within 5%. The meso-parameters of the final parallel bonding model are shown in Table 2.

Table 2 PFC2D simulation meso parameters

| | | | P | ar | P | ar | P | ar | P | ar |
|---|---|-----|-----|------|----|----|----|----|-----|-----|
| M | M | i | P | a | P | a | P | a | P | a |
| o | o | m | rti | cl | ti | rt | o | le | l | b |
| d | d | u | cl | C | cl | c | d | B | o | ral |
| e | e | m | e | o | e | l | r | n | n | lel |
| l | l | pa | ra | Part | nt | st | a | o | d | bo |
| h | l | rti | di | icle | a | if | fr | a | n | ta |
| w | w | cl | us | den | ct | f | i | d | nd | n |
| e | i | cl | us | den | ct | n | c | M | if | no |
| i | i | e | rat | sity | M | e | ti | u | f | rm |
| g | d | ra | io | p/(| o | s | d | o | n | e |
| g | t | ra | io | o | ss | o | f | d | al | nt |
| h | h | di | R | kg/ | d | ra | f | ul | e | str |
| t | h | us | m | m3) | ul | ra | a | u | ss | ess |
| L | W | R | ax | u | ti | f | c | ra | op | 1 |
| / | m | m | /R | s | o | a | t | ti | /M | st |
| m | m | in | mi | E | k | c | o | E | o | re |
| m | m | / | n | c/ | n/ | t | r | p/ | k | ss |
| | | | | G | k | o | λ | G | n/- | tp |
| | | | | P | s | r | a | P | k | M |
| | | | | a | μ | | | a | s | P |
| 1 | 5 | 3 | 1. | 283 | 1 | 2. | 0 | 1 | 1 | 1 |
| 0 | 0 | 66 | 0 | 5 | 5 | 5 | . | 5 | 5 | 5 |
| 0 | 0 | | | | | | | | | |

3. Orthogonal model tests for particle flow simulation of fractured granite

3.1 Design of orthogonal simulation test scheme

As a rule of thumb, the orthogonal test can select uniform discrete levels and representative factors to design the experiment, which can greatly reduce the experimental workload. In addition, variance analysis can also be used to analyze the influence of different factors on the dependent variable. Therefore, this paper adopts the orthogonal test to study the influence of single-crack geometric characteristics on the macro-mechanical properties of granite.

When carrying out the orthogonal test of the geometric characteristic parameters of the crack, we adopted a design scheme with 4 levels and 4 factors (shown as Table 3). The 4 factors are the geometric characteristic parameters of the crack, and the 4 levels are the values of the average discrete distribution of each geometric parameter. The primary crack geometric feature parameters include: ① Crack inclination angle x_1 , ② Crack length x_2 , ③ Crack X-axis position component x_3 , ④ Crack Y-axis position component x_4 ; The macro-mechanical parameters of rock samples considered include: ① peak strength y_1 , ② elastic modulus y_2 .

When the particle flow numerical simulation test is carried out, the correlation between the four factors is not considered, and the orthogonal table is used to obtain a specific test plan with four factors and four levels (show as Table 4). The inclination angle of the primary crack (that is, the angle between the crack direction and the X-axis direction) is set to four levels of 0, 30, 60 and 90 respectively; Considering the influence of specimen length, width and boundary mechanical effects, the crack lengths are set to four grades of 5, 10, 15 and 20 mm, respectively; Considering the axial symmetry of the specimen under uniaxial compression, a Cartesian coordinate system is established with the center of the specimen, which is divided into five equal parts from the origin of the X and Y axes to the boundary of the specimen, respectively. Take the middle 4 coordinate points as the values of the 4 levels of the X and Y axes, as shown in Table 4. Table 4 also lists the simulation results of macroscopic mechanical parameters (peak strength, elastic modulus) for each experiment.

Table 3 Orthogonal test level design table

| fa ct or le ve | Angl e x_1 ($^{\circ}$) | Crack length x_2 (mm) | X-axis components x_3 (mm) | Y-axis component x_4 (mm) |
|----------------------------|-----------------------------------|-------------------------------|------------------------------------|-----------------------------------|
| 1 | 0 | 5 | 5 | 10 |
| 2 | 30 | 10 | 10 | 20 |
| 3 | 60 | 15 | 15 | 30 |
| 4 | 90 | 20 | 20 | 40 |

Table 4 Granite particle flow orthogonal simulation test plan

| An gle x_1 ($^{\circ}$) | Crack length x_2 (mm) | Crack geometric feature parameters | | Macro- mechanical parameters | |
|--------------------------------------|----------------------------------|---------------------------------------|----------------------------------|--------------------------------------|---------------------------------------|
| | | x-axis compo x_3 (mm) | y-axis compo x_4 (mm) | peak intensi ty y_1 (MPa) | Elastic Modul us y_2 (MPa) |
| 0 | 5 | 5 | 10 | 48.5 | 30.1 |
| 0 | 10 | 20 | 30 | 37 | 28 |
| 0 | 15 | 10 | 40 | 30.7 | 26.7 |
| 0 | 20 | 15 | 20 | 29.7 | 22.2 |
| 30 | 5 | 15 | 30 | 41.1 | 29.1 |
| 30 | 10 | 10 | 10 | 40.2 | 27.2 |
| 30 | 15 | 20 | 20 | 38.8 | 27.4 |
| 30 | 20 | 5 | 40 | 29.8 | 23.5 |
| 60 | 5 | 20 | 40 | 39.6 | 28.1 |
| 60 | 10 | 5 | 20 | 47.9 | 29.8 |
| 60 | 15 | 15 | 10 | 37.2 | 26.4 |
| 60 | 20 | 10 | 30 | 32.6 | 28.1 |
| 90 | 5 | 10 | 20 | 51.2 | 31.2 |
| 90 | 10 | 15 | 40 | 50.9 | 31.1 |
| 90 | 15 | 5 | 30 | 50.8 | 30.8 |
| 90 | 20 | 20 | 10 | 50.3 | 30.9 |

3.2 Analysis of Numerical Simulation Test Results

Through the particle flow numerical simulation test, the macroscopic mechanical parameters of the rock are obtained, including ① peak intensity y_1 , ② elastic modulus y_2 , as shown in Table 5.

Table 5. Results of macro parameters

| numb er | peak intensity y_1 (MPa) | Elastic Modulus y_2 (MPa) |
|------------|-------------------------------|--------------------------------|
| 1 | 48.5 | 30.1 |
| 2 | 37 | 28 |
| 3 | 30.7 | 26.7 |
| 4 | 29.7 | 22.2 |
| 5 | 41.1 | 29.1 |
| 6 | 40.2 | 27.2 |
| 7 | 38.8 | 27.4 |
| 8 | 29.8 | 23.5 |
| 9 | 39.6 | 28.1 |
| 10 | 47.9 | 29.8 |
| 11 | 37.2 | 26.4 |
| 12 | 32.6 | 28.1 |
| 13 | 51.2 | 31.2 |
| 14 | 50.9 | 31.1 |
| 15 | 50.8 | 30.8 |
| 16 | 50.3 | 30.9 |

3.2.1 Analysis of variance

In this experiment, the effects of four mesoscopic parameters: ① crack inclination angle x_1 , ② crack length x_2 , ③ crack X-axis position component x_3 , and ④ crack Y-axis position component x_4 , on macro-mechanical

parameters of rock are discussed. Therefore, a multivariate analysis of variance is required.

SPSS software was used for multivariate analysis of variance. First, the model mode is selected to be customized, the interaction between factors is ignored, and the main effect of each factor is analyzed. Secondly, the significance level of the orthogonal test in this paper is selected as $\alpha = 0.05$, and the analysis results are shown in Table 6-Table 7.

Table 6 Analysis of variance of peak intensity

| source of variance | deviation sum of squares | degrees of freedom | sum of mean squares | F value | Significance |
|------------------------------|--------------------------|--------------------|---------------------|---------|--------------|
| Angle x_1 ($^{\circ}$) | 526.982 | 3 | 175.661 | 12.016 | 0.050 |
| Crack length x_2 (mm) | 230.437 | 3 | 76.812 | 5.317 | 0.100 |
| X-axis components x_3 (mm) | 71.092 | 3 | 23.697 | 1.640 | 0.347 |
| Y-axis components x_4 (mm) | 84.257 | 3 | 28.086 | 1.944 | 0.249 |
| e | 43.337 | 3 | 14.446 | | 0.9 |

Table 7. Analysis of variance of the elastic modulus

| source of variance | deviation sum of squares | degrees of freedom | sum of mean squares | F value | Significance |
|------------------------------|--------------------------|--------------------|---------------------|---------|--------------|
| Angle x_1 ($^{\circ}$) | 47.627 | 3 | 15.876 | 3.036 | 0.193 |
| Crack length x_2 (mm) | 27.788 | 3 | 9.263 | 1.771 | 0.252 |
| X-axis components x_3 (mm) | 5.148 | 3 | 1.716 | 0.328 | 0.080 |
| Y-axis components x_4 (mm) | 7.448 | 3 | 2.483 | 0.475 | 0.222 |
| e | 15.688 | 3 | 5.229 | | 0.0 |

According to the magnitude of the F statistic, the primary and secondary order of the influence of each factor on the macro-mechanical parameters of rock can be judged. It can be seen from Table 5 that the order of the influence of the crack geometric characteristic parameters on the peak strength is: crack inclination angle > crack length > Y-axis position component > crack X-axis position component. Among them, the crack inclination angle is the most significant influencing factor, followed by the crack length, the Y-axis position component and the X-axis position component of the grain. Due to the crack length, the Y-axis position component and the X-axis position component of the pattern, the deviation sum of the above three parameters is not lower than the experimental error. It shows that each parameter has a certain effect on the peak intensity, but has no significant effect. It can be seen from Table 6 that the order of influence of the crack geometric characteristic parameters on the elastic modulus is: crack inclination angle > crack length > Y-axis position component > crack X-axis position component. The crack inclination angle and crack length have a certain influence on the elastic modulus, but the influence is not significant.

From the above variance analysis results, it can be seen that the influence of the four meso-parameters on the macro-parameters is not the same. The crack inclination angle is a significant factor affecting the strength characteristics of rock, and the main influencing factor is the crack length.

3.2.2 Regression analysis

According to the calculation results of the above numerical simulation experiments, the relationship between the macro parameters and the main significant factors can be established. Using the stepwise regression method, the probability threshold value of variable entry is 0.05, and the probability threshold value of deletion is 0.10. A significance level of $\alpha = 0.05$ was taken as the standard for the regression coefficient test. The significant influencing factor of the peak strength is the crack inclination angle, and the linear regression analysis is carried out to obtain the formula (1). Its fitting coefficient is $R^2=0.648$.

$$y_1=0.169x_1+34.295$$

It can be seen from the above formula that the fitting coefficient of linear regression is small, and the fitting effect is relatively poor. It shows that the relationship between the meso-parameters and the crack inclination is complex, and there may be a nonlinear relationship. What kind of nonlinear relationship exists will be univariate analysis in the follow-up research.

4. Mechanical characteristics of fractured granite under the influence of single factor

4.1 Experimental Design

From a single factor (such as length, dip angle and location) to study the effect of crack geometry on the

macroscopic mechanical properties of granite, the tests are divided into three groups:①The crack is located in the center of the specimen, the length of the crack is 20 mm, and the angle between the crack direction and the X axis is set to 0, 15, 30, 45, 60, 75 and 90 respectively;②The crack is located in the center of the specimen, the angle between the crack direction and the X axis is 0, 15, 30, 45, 60, 75, 90, and the crack lengths are changed to 10 mm, 15 mm, 20 mm, 25 mm, 30 mm, and 35mm;③ The angle between the crack direction and the X axis is 45 mm, the crack length is 15 mm, and 4 positions are set as the crack center points. In order to avoid the adverse effect of the boundary effect on the rock fracture, the cracks are arranged within a reasonable size range [17].

4.2 Influence of crack inclination angle on rock strength

The crack inclination angle has a significant effect on the initiation position and failure mode of the new crack. Figure 3 shows the generation and expansion of new cracks caused by uniaxial compression in the simulated granite under the condition of different crack inclination angles at a certain number of calculation steps. It can be seen from the figure that when the crack inclination angle is 0, the crack initiation position is in the middle of the prefabricated crack. With the progress of the axial loading, the new cracks start from the middle and continue to expand to both ends of the specimen along the direction of external load (that is, the direction of maximum principal stress). The specimen is mainly dominated by tension cracks, and the crack tip is accompanied by local shear crack failure.

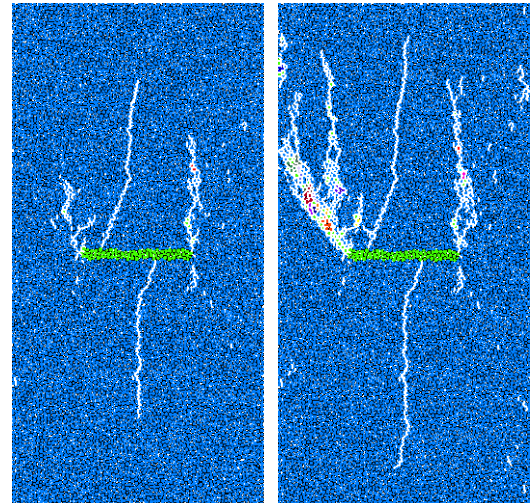
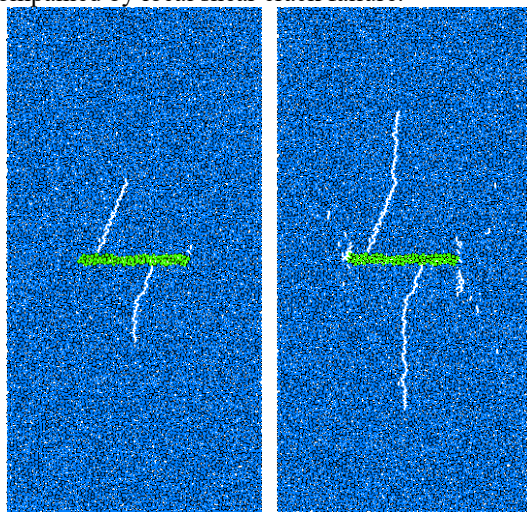
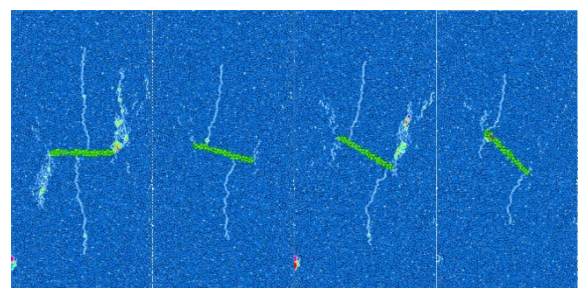


Fig.4 Uniaxial compression failure diagram of horizontal fracture

With the increase of the crack inclination angle, the crack initiation position of the new crack gradually shifts from the middle of the original crack to the crack tip. When the inclination angle of the primary crack is 15°, the crack initiation position is about 1/2 from the middle of the crack to the two ends. The new crack is dominated by tension and extends to both ends of the specimen along the external load direction; When the inclination angle of the primary crack is 30°, the crack initiation position is located at 2/3 of the middle of the primary crack, and the shear damage at the tip also increases gradually; When the inclination angle of the primary crack is 45°, the initiation position of the new crack is transferred to the tip of the primary crack, and the tensile failure and the local shear failure intersect each other; When the inclination angle of the primary crack is 60°, the specimen starts to be dominated by shear failure cracks, and accompanied by local tensile failure, the new cracks gradually expand along the tangential direction of the primary crack; When the inclination angle of the primary crack is 75°, an inclined shear crack penetrates the specimen along the direction of the primary crack and finally forms a fracture surface, which is a typical shear failure mode; When the inclination angle of the primary crack is 90°, a series of shear cracks are formed at the tip of the primary crack under the influence of shear stress, and the cracks gradually expand until they penetrate the boundary of the rock sample (Fig. 3a).



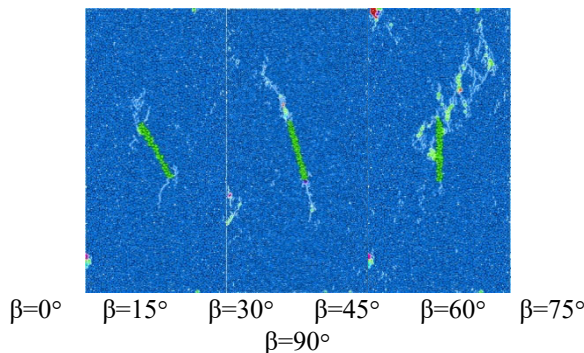


Fig.5 Distribution of new cracks in rock samples with different dip angles of primary microcracks under uniaxial compression

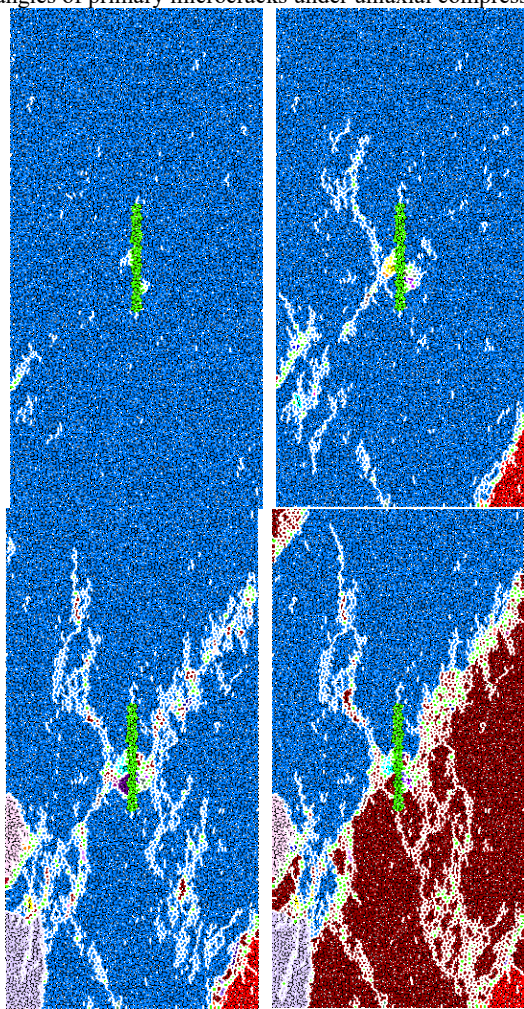


Fig.6 Uniaxial compression failure diagram of vertical fracture
Figure 4 shows the stress-strain relationship curve of rock caused by uniaxial compression under the condition of different inclination angles of primary cracks. It can be found that with the increase of the inclination angle of the primary crack in the rock, the uniaxial compressive strength of the rock increases continuously. When the inclination angle of the primary crack is 0° , the uniaxial compressive strength is the smallest, which is 29.6 MPa; Before the inclination angle of the primary crack increases to 30° , the upward trend of the peak value is relatively gentle; When the inclination angle increases to 45° , the peak value increases to 39.5 MPa, and the peak intensity is 15.8% higher than that of 30° ; When the

inclination angle of the primary crack increases from 45° to 90° , the peak strength increases to 53.4 MPa. Compared with the original crack inclination angle of 45° , the peak strength is increased by 35.2%. Compared with the obvious increase from 0 to 45° , it can be seen that 45° is the dividing point of the peak intensity increase rate. When the inclination angle of the primary crack is less than 45° , the peak strength of the rock rises gently. After the inclination angle of the primary crack reaches 45° , the peak strength of the rock increases rapidly, which is consistent with the research of other scholars.

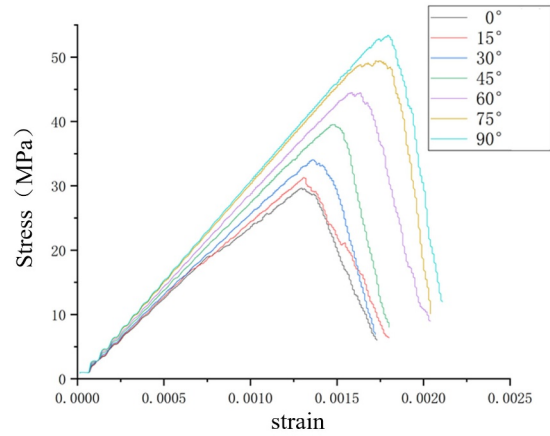


Fig.7 Stress-strain curves of specimens with cracks at different inclination angles

4.3 Influence of primary crack length and dip angle on rock strength

Fig. 5 shows the uniaxial compressive strength curves of rock samples with different dip angles and lengths of primary cracks. It can be seen from the figure that under the condition that the inclination angle of the primary crack remains unchanged, except for the case where the inclination angle is 90° , the peak strength of the rock sample basically shows a decreasing trend with the increase of the primary crack length. For example, when the inclination angle of the primary crack is 0° , the peak strength of the rock sample is reduced by 81.2% when the primary crack length is 35 mm and the crack length is 10 mm. However, when the inclination angle of the primary crack is 90° , that is, when the direction of the crack is consistent with the direction of force loading, the peak strength of the rock sample basically does not change with the increase of the crack length. The inclination angle of the primary crack is positively correlated with the peak strength of the rock sample, which means that the larger the crack inclination angle, the higher the peak strength of the rock sample. When the primary crack length is 10 mm, the peak strength of the rock sample when the crack inclination angle is 0° is 38 MPa, however, under the condition of the same crack length, when the crack inclination angle is 90° , the peak strength of the rock sample is 55 MPa. It can be seen that the inclination angle of the primary crack and the length of the crack in the rock sample have a greater influence on the peak strength of the rock sample. The smaller the crack inclination angle and the longer the length, the lower the peak intensity of the rock sample.

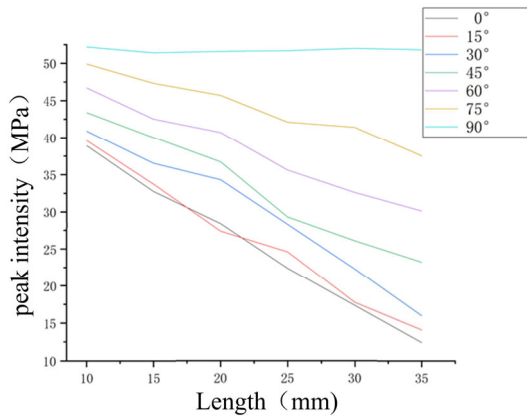


Fig. 8 Variation curve of peak strength of specimen under cracks with different inclination angles and lengths

4.4 Influence of crack position on rock peak strength

Since the uniaxial compression test is axisymmetric, a numerical simulation experiment of the failure evolution of rock samples under uniaxial compression conditions with primary cracks at four different positions is designed in this paper (Fig. 9). That is, the midpoint coordinates of the primary crack are located at point 1 (x_4, y_2) , point 2 (x_2, y_2) , point 3 (x_4, y_4) , and point 4 (x_2, y_4) .

Figure 7 shows the peak intensity of the rock samples when the primary cracks are in 4 different positions, and the difference between them is relatively small, ranging from 2 to 4 MPa.Compared with the peak intensity of relatively complete rocks, the intensity decreases between 23% and 31%, and the peak intensity generally shows a trend of high in the middle and low in the surrounding area.From the point of view of the failure form of the rock sample, when the primary crack is close to the edge of the rock sample (point 3), the crack is more likely to penetrate to the boundary, resulting in a significant decrease in the peak strength of the rock sample.

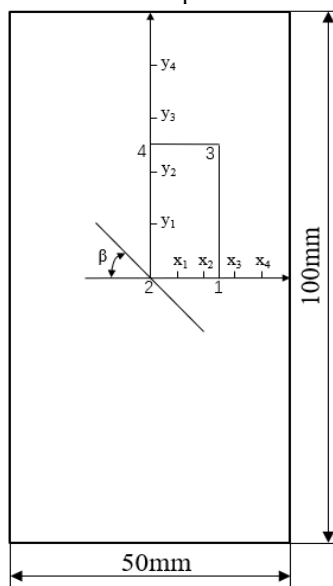


Fig.9 Schematic diagram of crack center position distribution

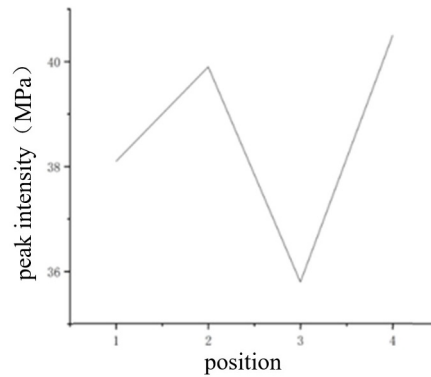


Fig.10 Peak intensity change curves at different positions

Figure 11 shows the effect of primary crack location on the stress-strain relationship of rock samples in uniaxial compression experiments. It can be seen that the location of the primary crack mainly changes the peak intensity of the rock sample and the stress-strain state after the peak, but has no significant effect on the elastic modulus of the rock sample (that is, the slope of the straight line in the stress-strain relationship curve).

The characteristics of the stress-strain relationship curve are mainly as follows:1) When the primary crack is located in the middle of the rock sample (point 2 and point 4), there is only one peak strength, and the stress of the rock sample falls back rapidly after the peak, which is consistent with the stress-strain relationship curve of the classical general rock;2) When the primary crack is located at the edge of the rock sample (such as point 3), the post-peak stress of the rock sample falls back slowly. And after the stress reaches the first peak strength (that is, the uniaxial compressive strength), there is a small increase after the post-peak stress has a large fall back; When the primary crack is located at the lateral boundary in the middle of the rock sample (such as point 1).After the stress first reached its peak, it did not fall back rapidly, but with the continuous fluctuation of the stress, a larger peak strength appeared than that in the linear elastic stage.where the second peak strength is the uniaxial compressive strength.

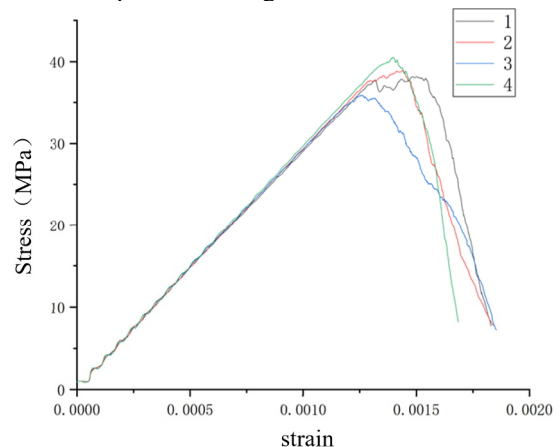


Fig.11 Stress-strain curves of specimens at different positions

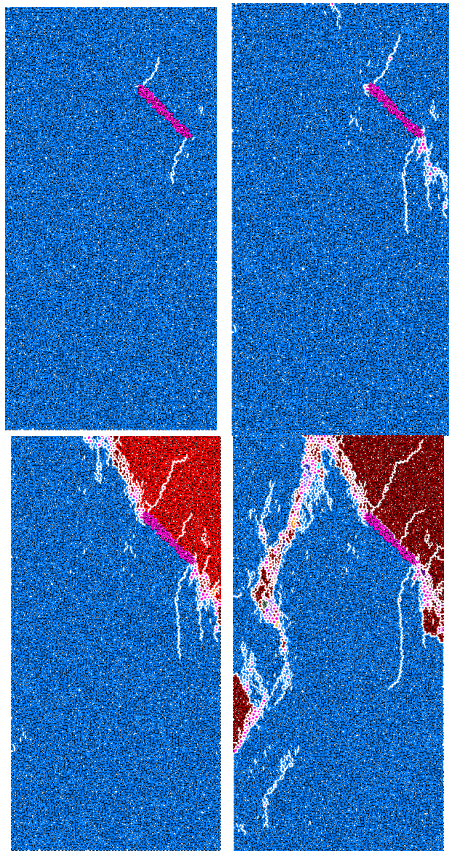


Fig.12 The fracture process of fractured rock at the same location

5. Conclusion

When the crack inclination angle is 0° , the crack initiation position is in the middle of the prefabricated crack, and gradually moves to both ends of the crack as the angle increases. With the continuous loading, the crack starts from the middle and expands to both ends of the specimen along the direction of external load. The specimen is mainly composed of tension cracks, and the crack tip is damaged by local shear cracks; The longer the crack length, the lower the peak strength and the worse the stability. The change of crack position mainly changed the peak strength and post-peak stress-strain state of the rock sample, but had no obvious effect on the elastic modulus.

2) The influence of the crack geometric characteristic parameters on the peak strength is as follows: the position component of the Y axis of the crack > the position component of the X axis of the crack > the length of the crack > the inclination angle of the crack. The influence of the position offset in the normal direction of the loading axis, and the influence of the position offset along the crack (X, Y axis) on the peak strength are also much greater than the effects of the crack length and inclination angle.

3) The influence of the crack geometric characteristic parameters on the elastic modulus is as follows: the position component of the X axis of the crack > the position component of the Y axis of the crack > the length of the crack > the inclination angle of the crack, and the position offset of the crack along the normal direction of

the loading axis affects the elastic modulus It is slightly larger than the influence of the position offset of the crack along the loading axis, and the influence of the position offset of the crack (X, Y axis) on the elastic modulus is also much greater than that of the crack length and inclination angle.

References

1. Zhang Guokai, Li Haibo, Wang Mingyang, Li Xiaofeng. Study on crack propagation characteristics of single-fracture rock based on acoustic test and camera technology [J]. Geotechnical Mechanics, 2019, 40(S1): 63-72+81.
2. Xiao Taoli, Li Xinping, Jia Shapo. Triaxial test study and mechanical analysis of structural plane effect of deep single-fracture rock mass [J]. Chinese Journal of Rock Mechanics and Engineering, 2012, 31(08): 1666-1673.
3. Zhou Hui, Meng Fanzhen, Zhang Chuanqing, Lu Jingjing, Xu Rongchao. Experimental study on the effect of fractures of different positions and sizes on rock mass failure [J]. Chinese Journal of Rock Mechanics and Engineering, 2015, 34(S1): 3018-3028.
4. Liu Hongyan, Huang Yushi, Li Kaibing, Zhang Jihong. Experimental study on strength and failure mode of prefabricated jointed rock mass specimens [J]. Rock and Soil Mechanics, 2013, 34(05): 1235-1241+1246.
5. Ke Zhiqiang, Wang Huanling, Xu Weiya, Lin Zhinan, Ji Hua. Experimental study on mechanical properties of columnar jointed rock mass with lateral joints [J]. Rock and Soil Mechanics, 2019, 40(02): 660-667.
6. Guo Qifeng, Wu Xu, Cai Meifeng, Xi Xun, Ren Fenhua, Miao Shengjun. Strength characteristics and failure mode test of prefabricated fractured granite [J]. Journal of Engineering Science, 2019, 41(01): 43-52.
7. Yin Qian, Jing Hongwen, Su Hajian, Zhao Honghui. Strength degradation and loading rate effect of sandstone with longitudinal fractures [J]. Chinese Journal of Mining and Safety Engineering, 2016, 33(01): 128-133.
8. Wang Guoyan, Yu Guangming, Song Chuanwang. Influence of geometric elements of initial fissures on the evolution of rock fissures [J]. Journal of Liaoning University of Engineering and Technology (Natural Science Edition), 2011, 30(05): 681-684.
9. Shi Chong, Xu Weiya. Numerical simulation skills and practice of particle flow [M]. Beijing: China Construction Industry Press, 2015
10. Huang Yanhua, Yang Shengqi. Particle flow simulation of macro-mechanical behavior of non-coplanar double-fractured red sandstone [J]. Chinese Journal of Rock Mechanics and Engineering, 2014, 33(08): 1644-1653.
11. Chen Pengyu. Research status of PFC~(2D) simulation of crack propagation characteristics of

- fractured rocks [J]. Chinese Journal of Engineering Geology, 2018, 26(02): 528-539.
- 12. Yuan Guangxiang, Zhang Luqing, Zeng Qingli, Li Jianyong, Huang Zhiqian, Wang Hongjian, Deng Xubiao. Study on the correlation between mineral composition of granite and its uniaxial compressive strength [J]. Hydrogeology and Engineering Geology, 2018, 45(05): 93-100.
 - 13. Budong Yang, Yue Jiao, Shuting Lei. A study on the effects of microparameters on macroproperties for specimens created by bonded particles[J]. Engineering Computations: International Journal for Computer-Aided Engineering and Software, 2006, 23(6).
 - 14. D.O. Potyondy, P.A. Cundall. A bondedparticle model for rock[J]. International Journal of Rock Mechanics and Mining Sciences, 2004, 41(8).
 - 15. Zhao Guoyan, Dai Bing, Ma Chi. Study on the influence of mesoscopic parameters on macroscopic properties in the parallel bonding model.
 - 16. Jiang Mingjing, Fang Wei, Sima Jun. Microparameter calibration of parallel bonding model for simulated rock [Xiao.Journal of Shandong University (Engineering Edition). 2015,45(04):50-56.
 - 17. Fu Zhen, Cai Yongen. Numerical analysis of the effect of rock specimen size on crack stress field [J]. Chinese Journal of Seismology, 2005(03):301-308+355.